Inorg. Chem. **2008**, *47*, 5720−5726

Detailed Magnetic Studies on $Co(N_3)_2(4\text{-acetylpyridine})_2$: a Weak-Ferromagnet with a Very Big Canting Angle

Xin-Yi Wang, Zhe-Ming Wang, and Song Gao*

Beijing National Laboratory for Molecular Sciences, State Key Laboratory of Rare Earth Materials Chemistry and Applications, College of Chemistry and Molecular Engineering, Peking University, Beijing 100871, P.R. China

Received December 3, 2007

The magnetic properties of $Co(N_3)_2(4acpy)_2$ have been thoroughly reexamined on both powder and well-oriented single crystal samples. This azido-bridged cobalt compound of (4, 4) layer shows a weak-ferromagnetic state below $T_C = 11.2$ K. The magnetic axes were determined to be along the crystallographic *a**, *b*, and *c* axes for the monoclinic space group $P2_1/c$. The easy axis lies along the *b*-axis, the canting is along the *a**-axis, and the hard axis is along the *c*-axis. Strong anisotropy due to the oriented moments in the ordered state and/or the single-ion anisotropy of Co^{2+} exists in the whole temperature range from 2 to 300 K. Below T_C, very big spontaneous magnetization was observed and was attributed to the very big canting angle (15° at 2 K). A possible spin configuration was then proposed to explain the experimental results. The origin of the big spin canting was discussed, and a weak-ferromagnetic approach toward molecular magnets with big spontaneous magnetization was proposed accordingly.

Introduction

Numerous scientific endeavors have been focused on molecular magnets recently because of their theoretical and practical importance.[1] For future applications, molecular magnets with big and permanent spontaneous magnetization are a continuing pursuit. Generally, two approaches, ferro- and ferrimagnetic (*FO* and *FI*), can lead to this purpose. Because of the parallel alignment of the moments, the ferromagnets naturally have high spontaneous magnetization. The *orthogonal magnetic orbital*[2] and *spin polarization*[3] were proposed to realize the *FO* interaction and resulted in a number of molecular ferromagnets.[4] However, because of the infrequence and weakness of the *FO* interaction compared to the antiferromagnetic (*AF*) interaction, ferromagnets were somewhat limited and more attention has been paid to the *FI* systems ever since it was first realized by Neél, the 1970 Nobel Laureate in physics, in his famous studies of garnets and spinel ferrites. In molecular magnetism, the *FI* approach, with careful design of magnetic interaction of spins and controllable synthesis, was then developed by Verdaguer and Kahn et al. in their *FI* chain compounds $MnCu(dto)_2(H_2O)_3\cdot 4.5H_2O$[5] and $MnCu(pbaOH)(H_2O)_3$[6] and then demonstrated well in the cyanide-bridged systems. In fact, most high-T_c molecular magnets, for example, $K_{0.5}V^{II/III}[Cr(CN)_6]_{0.95}\cdot 1.7H_2O$ ($T_c = 350$ K) and $KV^{II}[Cr(CN)_6]\cdot 2H_2O$ ($T_c = 376$ K), are ferrimagnets.[7]

On the other hand, in the *AF* coupled system, the weak-ferromagnets due to spin canting also have spontaneous magnetization and are efficient to construct molecular magnets.[8–19] Because the canting angle (γ) is usually small

* To whom correspondence should be addressed. E-mail: gaosong@pku.edu.cn.

(1) (a) *Molecular Magnetism: From Molecular Assemblies to the Device*, NATO ASI Series E, Vol. 321; Coronado, E., Delhaes, P., Gatteschi, D., Miller, J. S., Eds.; Kluwer: Dordrecht, 1995. (b) *Magnetism: Molecules to Materials*; Miller, J. S., Drillon, M., Eds.; Wiley-VCH: New York, 2002− 2005; Vols. I-IV.
(2) (a) Goodenough, J. B.; Loeb, A. L. *Phys. Rev.* **1955**, *98*, 391. (b) Goodenough, J. B. *Phys. Rev.* **1956**, *100*, 564. (c) Kanamori, J. *Prog. Theor. Phys.* **1957**, *17*, 177.
(3) McConnell, H. M. *J. Chem. Phys.* **1963**, *39*, 1910.
(4) Kahn, O. *Molecular Magnetism*; VCH: New York, 1993; Chapters 8, 12.
(5) (a) Verdaguer, M.; Gleizes, A.; Renard, J. P.; Seiden, J. *Phys. Rev. B* **1984**, *29*, 5144. (b) Gleizes, A.; Verdaguer, M. *J. Am. Chem. Soc.* **1984**, *106*, 3727.
(6) Kahn, O.; Pei, Y.; Verdaguer, M.; Renard, J. P.; Sletten, J. *J. Am. Chem. Soc.* **1988**, *110*, 782.
(7) (a) Holmes, M. S.; Girolami, G. S. *J. Am. Chem. Soc.* **1999**, *121*, 5593. (b) Manriquez, J. M.; Yee, G. T.; Mclean, R. S.; Epstein, A. J.; Miller, J. S. *Science* **1991**, *252*, 1415. (c) Ferlay, S.; Mallah, T.; Quahes, R.; Veillet, P.; Verdaguer, M. *Nature* **1995**, *378*, 701.
(8) Carlin, R. L. *Magnetochemistry*; Springer-Verlag: Berlin, Germany, 1986.
(9) (a) Moriya, T. *Phys. Rev.* **1960**, *120*, 91. (b) Moriya, T. *Phys. Rev.* **1960**, *117*, 635. (c) Dzialoshinski, I. *J. Phys. Chem. Solids* **1958**, *4*, 241.

10.1021/ic7023549 CCC: $40.75
Published on Web 06/05/2008

(a few degrees or less), most of the weak-ferromagnets do not have large spontaneous magnetization. However, a large net moment could be generated by spin-canting as long as the canting angle γ is big enough. For example, when γ is 20°, the resulting net moment could be as large as 34.2% (sin 20°) of the total spin. This is even more efficient than the *FI* alignment of two heterospins with *S* and 2*S* (the net moment is *S*, 33.3% of the total). Among the reported molecular weak-ferromagnets, those with big canting angles are still limited. $Co(N_3)_2(bpg)_2$[10a] ($\gamma = 5.2°$), $Fe(N_3)_2$(4,4′-bipyridine)[11] ($\gamma \approx 7-8°$), $Fe(dca)_2$[12] ($\gamma = 7.2°$), $Fe(pyrimidine)_2Cl_2$[14] ($\gamma = 14°$), $Co(pyrimidine)_2X_2$[15] ($X = Cl^-$ and Br^-, $\gamma \approx 9°$), Mn(cyclam)$(SO_4)(ClO_4)(H_2O)$[16] ($\gamma = 8.4°$), Mn(cyclam)$(HCOO)(CF_3SO_3)(ClO_4)$ ($\gamma = 4.8°$),[16] and $[Mn(TPP)O_2PHPh]\cdot H_2O$[17] ($\gamma = 34.6°$) are a few of the limited examples. For the compound $[Mn(TPP)O_2PHPh]\cdot H_2O$, the noncompensated spins due to spin canting result in a very interesting single chain magnetic behavior. Interestingly, in all these materials, two important common characters exist: spin centers with large anisotropy (Co^{2+}, Fe^{2+}, and Mn^{3+}) and asymmetric three-atom bridges (N_3^-, 1,3-dca, $HCOO^-$, pyrimidine, and RPO_2^-). This fact prompts us to the further investigation of the $Co^{2+}-N_3^-$ system after our former results on $Co(N_3)_2(bpg)_2$. Presented here is a simple yet interesting compound, $Co(N_3)_2(4acpy)_2$ (**1**, 4acpy = 4-acetylpyridine). During the course of preparation of this manuscript, the crystal structure and magnetic behavior of this compound were reported by Vicente and co-workers,[20] who concluded that the material undergoes a transition to long-range magnetic ordering below 25 K. However, they overestimated the ordering temperature, and no anisotropic results were reported because the magnetic studies were carried on powder samples. Here, we report the detailed magnetic measurements on both powder and single crystal samples of **1**. Our results reveal a very big canting angle ($\gamma \approx 15°$) in the weak-ferromagnetic state of **1**. A possible spin configuration in the ordered state was proposed. In addition, a weak-ferromagnetic approach toward molecular magnets with big spontaneous magnetization was proposed. These thorough studies show the great importance of the anisotropic measurements on single crystals for a better understanding of the magnetic properties.

Experimental Section

General Remarks. All starting materials were commercially available, reagent grade, and used as purchased without further purification. Elemental analysis of carbon, hydrogen, and nitrogen was carried out with an Elementary Vario EL. The microinfrared spectroscopy study was performed on a Magna-IR 750 spectrophotometer in the 4000−500 cm^{-1} region. Variable-temperature magnetic susceptibility (2−300 K) and field dependence of magnetization (−5 to +5 T) on a polycrystalline sample and on carefully oriented single crystals (two single crystals of the mass of 0.78 and 0.22 mg were used because of the breaking of the single crystal during the measurement operations; the morphologies of these were determined using the single crystal X-ray diffraction) were performed on a Quantum Design MPMS XL-5 SQUID system equipped with a horizontal rotator sample holder. The orientation accuracy of the axes was estimated within several degrees during the measurements. All experimental magnetic data except for the rotation data were corrected for the diamagnetism of the sample holders and of the constituent atoms (Pascal's tables).

Caution! *Azide compounds are potentially explosive. Only a small amount of materials should be handled carefully.*

Synthesis of 1. A 6 mL volume of water solution containing $CoCl_2\cdot 6H_2O$ (72 mg, 0.30 mmol) and NaN_3 (39 mg, 0.60 mmol) was added slowly to 6 mL of methanol solution containing the 4acpy (72 mg, 0.60 mmol) and filtrated. Slow evaporation for 4 days gave plate-like red crystals (up to 4.0 × 4.0 × 0.5 mm^3) of **1** in yield of 70%. Anal. (%) Calcd for $C_{14}H_{14}N_8O_2Co$: C, 43.65; N, 29.09; H, 3.66. Found: C, 43.81; N, 29.53; H, 3.56. IR(microspectrum, cm^{-1}): 2073s and 2096s for azido.

Structure Determination. The data were collected on a Nonius Kappa CCD with Mo Kα radiation ($\lambda = 0.71073$ Å) at 293 K. The structure was solved by direct methods and refined with full-matrix least-squares on F^2 using the SHELX-97 program. All non-hydrogen atoms were refined anisotropically. Crystal data of **1**, $C_{14}H_{14}N_8O_2Co$, $M_r = 385.26$, monoclinic, space group $P2_1/c$, $a = 11.7309(4)$, $b = 8.3099(2)$, $c = 8.2315(2)$ Å, $\beta = 92.350(1)°$, $V = 801.75(4)$ Å^3, $z = 2$, μ(Mo Kα) = 1.098 mm^{-1}, GoF = 1.098. A total of 15920 reflections were collected and 1835 are unique. *R*1 and *wR*2 are 0.0259 and 0.0709, respectively, for 116 parameters and 1213 reflections [$I > 2\sigma(I)$]. CCDC-644780 contains the supplementary crystallographic data for this paper. It can be obtained free of charge from the Cambridge Crystallographic Data Centre via www.ccdc.cam.ac.uk/data_request/cif. Also, the CIF file for **1** can be found in the Supporting Information.

Result and Discussion

Structure of 1. The crystal structure of **1** has been previously reported.[20] For the completeness of this work and also for a better description of its magnetic properties, we briefly describe its structure here. It is a two-dimensional

(10) (a) Wang, X. Y.; Wang, L.; Wang, Z. M.; Gao, S. *J. Am. Chem. Soc.* **2006**, *128*, 674. (b) Wang, X. Y.; Wang, L.; Wang, Z. M.; Su, G.; Gao, S. *Chem. Mater.* **2005**, *17*, 6369.

(11) Fu, A. H.; Huang, X. Y.; Li, J.; Yuen, T.; Lin, C. L. *Chem.—Eur. J.* **2002**, *8*, 2239; The authors attributed its magnetic ground state to some ferromagnetic state, but we think it is also a weak-ferromagnet.

(12) (a) Batten, S. R.; Murray, K. S. *Coord. Chem. Rev.* **2003**, *246*, 103. (b) Lappas, A.; Wills, A. S.; Prassides, K.; Kurmoo, M. *Phys. Rev. B* **2003**, *67*, 144406.

(13) (a) Kmety, C. R.; Huang, Q.; Lynn, J. W.; Erwin, R. W.; Manson, J. L.; McCall, S.; Crow, J. E.; Stevenson, K. L.; Miller, J. S.; Epstein, A. J. *Phys. Rev. B* **2000**, *62*, 5576. (b) Kurmoo, M.; Kumagai, H.; Green, M. A.; Lovett, B. W.; Blundell, S. J.; Ardavan, A.; Singleton, J. *J. Solid State Chem.* **2001**, *159*, 343.

(14) Feyerherm, R.; Loose, A.; Ishida, T.; Nogami, T.; Kreitlow, J.; Baabe, D.; Litterst, F. J.; Süllow, S.; Klauss, H. H.; Doll, K. *Phys. Rev. B* **2004**, *69*, 134427.

(15) Nakayama, K.; Ishida, T.; Takayama, R.; Hashizume, D.; Yasui, M.; Iwasaki, F.; Nogami, T. *Chem. Lett.* **1998**, 497.

(16) Mossin, S.; Weihe, H.; Sørensen, H. O.; Lima, N.; Sessoli, R. *Dalton Trans.* **2004**, 632.

(17) Bernot, K.; Luzon, J.; Sessoli, R.; Vindigni, A.; Thion, J.; Richeter, S.; Leclercq, D.; Larionova, J.; van der Lee, A. *J. Am. Chem. Soc.* **2008**, *130*, 1619.

(18) (a) Wang, X. Y.; Gan, L.; Zhang, S. W.; Gao, S. *Inorg. Chem.* **2004**, *43*, 4615. (b) Wang, X. Y.; Wei, H. Y.; Wang, Z. M.; Chen, Z. D.; Gao, S. *Inorg. Chem.* **2005**, *44*, 572. (c) Wang, Z. M.; Zhang, B.; Inoue, K.; Fujiwara, H.; Otsuka, T.; Kobayashi, H.; Kurmoo, M. *Inorg. Chem.* **2007**, *46*, 437.

(19) (a) Zeng, M. H.; Zhang, W. X.; Sun, X. Z.; Chen, X. M. *Angew. Chem., Int. Ed.* **2005**, *44*, 3079. (b) Rodríguez, A.; Kivekäs, R.; Colacio, E. *Chem. Commun.* **2005**, 5228. (c) Coronado, E.; Galán-Mascarós, J. R.; Gómez-García, C. J.; Murcia-Martínez, A. *Chem.—Eur. J.* **2006**, *12*, 3484. (d) Ouellette, W.; Prosvirin, A. V.; Chieffo, V.; Dunbar, K. R.; Hudson, B.; Zubieta, J. *Inorg. Chem.* **2006**, *45*, 9346.

(20) Abu-Youssef, M. A. M.; Mautner, F. A.; Vicente, R. *Inorg. Chem.* **2007**, *46*, 4654.

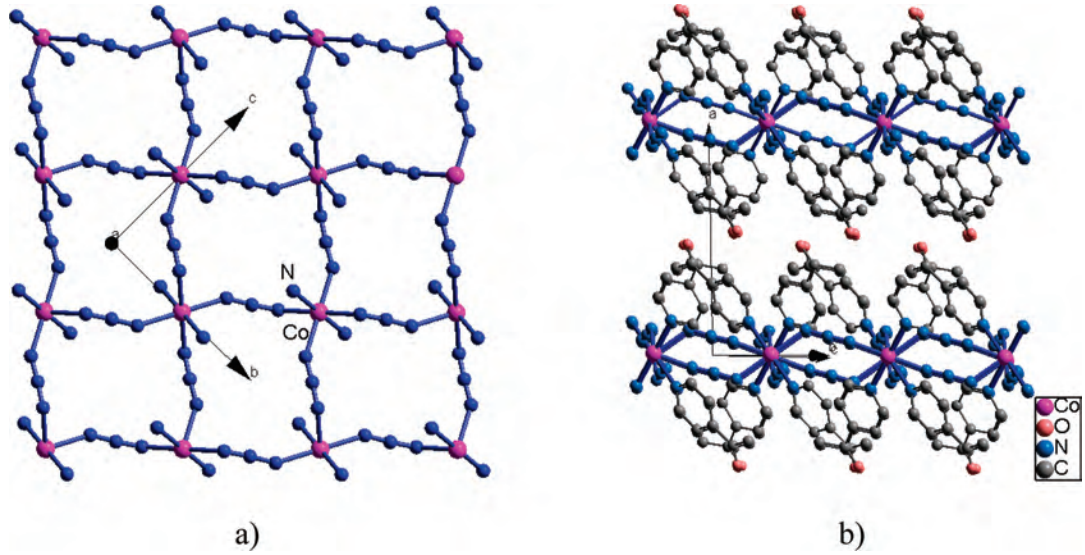

Figure 1. (4, 4) layer of **1** with Co^{2+} bridged by *EE*-azido (a) and its three-dimensional structure showing the packing of the layers (b).

(4, 4) layer with Co^{2+} bridged by *EE* azido (Figure 1a). Although it is common for Mn^{2+} and Ni^{2+},[21] **1** is the second cobalt compound with this layer besides $Co(N_3)_2(bpg)$.[10a] The unique Co^{2+} center sits in the inversion center and is octahedrally coordinated by six N atoms, four equatorial from the *EE* azides ($Co-N_{azido} = 2.125$ and 2.133 Å) and two apical from two *trans*-4acpy ligands ($Co-N_{acpy} = 2.172$ Å). The angles ∠N−Co−N are very close to 90° (from 88.2 to 91.8°), resulting in a regular octahedron slightly elongated along $N_{acpy}-Co-N_{acpy}$. This octahedral environment retains the approximate O_h point group and cannot quench efficiently the orbital moment of Co^{2+} and should lead to a big orbital residue, spin−orbital coupling, and anisotropy, which will greatly influence its magnetic property.[8,22] Bridged by *EE* azido, the Co^{2+} ions form an almost perfect square network along the *bc* plane with a unique Co···Co distance of 5.848 Å. The coordinated 4acpy molecules stick out of the plane, and there are no other evident interactions stronger than the van der Waals force between the layers (the shortest interlayer C···O contact is 3.43 Å, Figure 1b). The shortest interlayer Co−Co distance is 11.73 Å. The long interlayer distance suggests that the magnetic exchange between the layers will be very weak, most likely through dipole−dipole interaction. Because of the lack of an inversion center between adjacent spins and the tilting of the long axes of adjacent CoN_6 octahedra (the torsion angle of $N_{acpy}-Co-Co-N_{acpy}$ is 62.3°), weak-ferromagnetism due to spin-canting is allowed.[8,9]

Magnetic Properties

dc Measurements on a Powder Sample. The powder sample of **1** was first investigated magnetically and the results are mostly consistent with previously reported results.[20] As shown in Figure 2, upon cooling, $\chi_m T$ decreases slowly from 3.09 $cm^3\ mol^{-1}$ K at 300 K to a minimum of 2.02 $cm^3\ mol^{-1}$ K at 32 K, and then abruptly increases about 10 times at 10 K, after that it drops till 2 K. The Curie−Weiss fitting of χ_m^{-1} data above 80 K provides $C = 3.55$ $cm^3\ mol^{-1}$ K and $\theta = -45.4$ K, slightly higher than the reported 3.07 $cm^3\ mol^{-1}$ K and −22.7 K for **1**. These differences might come from the orientation of the sample during the measurements. Nevertheless, these results indicate strong *AF* coupling through the *EE* azido and the strong spin−orbital coupling of the ^4T_g state, consistent with the observed *AF* coupling in other $Co^{2+}-N_3^-$ compounds.[10a,23] The sharp peak at 10 K suggests the presence of spontaneous magnetization, which was further confirmed by the magnetization measurement at 2 K (inset of Figure 2). *M* increases quickly at very low field, reaching 0.66 μ_B at 400 Oe, and then increases slowly to 1.12 μ_B at 50 kOe, much less than the common value of 2−3 μ_B for a Co^{2+} center (at 2 K, the effective spin is $S = 1/2$ with a common value of *g* about 4.3). Furthermore, a square hysteresis loop at 2 K and sharp

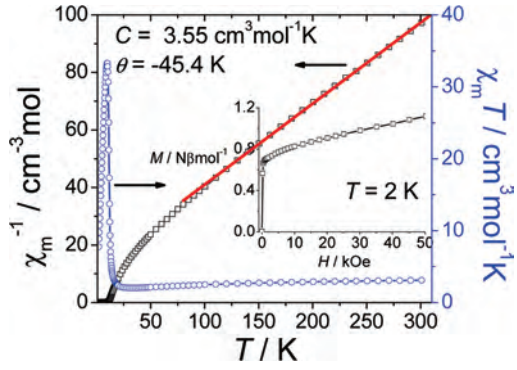

Figure 2. Temperature dependencies of χ_m^{-1} and $\chi_m T$ under $H = 1$ kOe. The red line is the Curie−Weiss fit. Inset: field dependent magnetization $M(H)$ at 2 K. All these data were for a powder sample of **1**.

(21) Ribas, J.; Escuer, A.; Monfort, M.; Vicente, R.; Cortés, R.; Lezama, L.; Rojo, T. *Coord. Chem. Rev.* **1999**, *1027.*, 193–195.

(22) (a) Figgis, B. N.; Gerloch, M.; Lewis, J.; Mabbs, F. E.; Webb, G. A. *J. Chem. Soc. A.* **1968**, 2086. (b) Aromí, G.; Stoeckli-Evans, H.; Teat, S. J.; Cano, J.; Ribas, J. *J. Mater. Chem.* **2006**, *16*, 2635. (c) Ostrovsky, S. M.; Falk, K.; Pelikan, J.; Brown, D. A.; Tomkowicz, Z.; Haase, W. *Inorg. Chem.* **2006**, *45*, 688.

(23) (a) Viau, G.; Lombardi, M. G.; De Munno, G.; Julve, M.; Lloret, F.; Faus, J.; Caneschi, A.; Clemente-Juan, J. M. *Chem. Commun.* **1997**, 1195. (b) Hernández, M. L.; Barandika, M. G.; Urtiaga, M. K.; Cortés, R.; Lezama, L.; Arriortua, M. I. *Dalton Trans.* **2000**, 79. (c) Doi, Y.; Ishida, T.; Nogami, T. *Bull. Chem. Soc. Jpn.* **2002**, *75*, 2455.

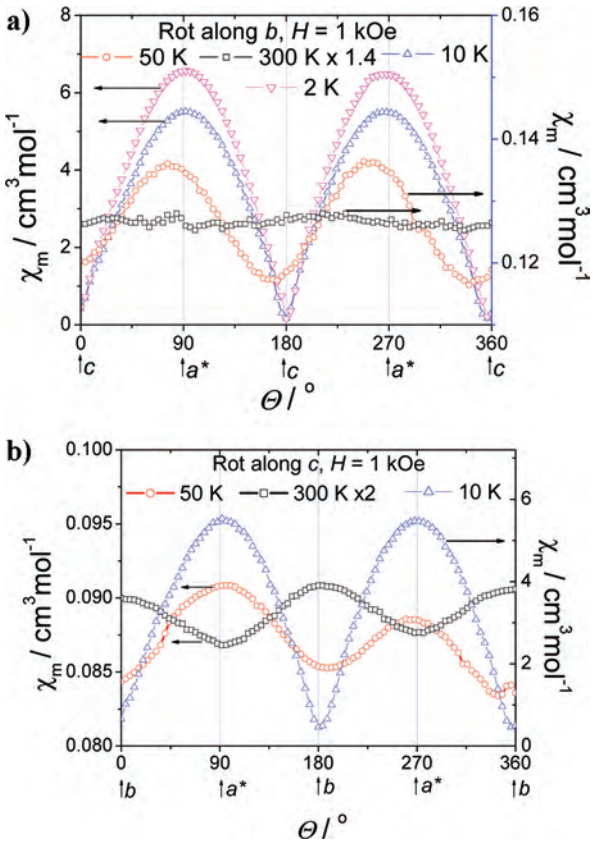

Figure 3. Angular dependences of the susceptibility of **1** under 1 kOe in the a^*c plane ((a), $\Theta = 0°$, H // c) and a^*b plane ((b), $\Theta = 0°$, H // b) at different temperatures.

peaks in both the in- and out-of-phase signals of the zero-field ac susceptibility, can also be observed and will be presented below together with the results on the single crystal of **1.**

Magnetic Studies on Single Crystals of 1

Determination of the Magnetic Axes. Because the space group of **1** is $P2_1/c$, the 2-fold axis of the monoclinic lattice, b, is necessarily one of the magnetic axes.[24] The other two magnetic axes may then be determined from the extremes of the magnetization in the ac plane with the crystal rotating along the b axis. As can be seen from the results measured in 1 kOe at 2, 10, 50, and 300 K (using the single crystal of 0.22 mg, Figure 3a), these extremes were found to be roughly along the a^* ($\Theta = 90°$ and 270°, maxima) and c ($\Theta = 0°$ and 180°, minima) directions at 2, 10, and 50 K.[25] At 300 K, there is no significant anisotropy in the ac plane. It should be noted here that the a^* axis is perpendicular to the (4,4) layers as they are parallel to the bc plane. We also performed the rotation measurements around the c axis at different temperatures (10, 50, and 300 K, using the single crystal of 0.78 mg, Figure 3b). Similarly, the extremes were observed along the a^* and b axes. At 300 K, the maxima are along b axis, and the minima along a^* axis. Interestingly, the situation is changed when the temperature decreases, with $\chi_m{}^{a^*}$ becoming the maximum at 50 and 10 K, where $\chi_m{}^{a^*}$ is almost ten times larger than $\chi_m{}^b$, indicating the strong magnetic anisotropy. We have to emphasize that cross comparison of the absolute values of the susceptibilities for the rotation data in Figure 3 (especially those at 300 K) is meaningless because of the noncorrected diamagnetic contribution from the rotator sample holder and the M-grease to hold the crystals. From both of these rotation measurements, we can come to the following conclusions: (1) the crystallographic axes a^*, b, and c are the magnetic axes; (2) strong magnetic anisotropy, originating from the single-ion anisotropy of the octahedral Co^{2+} centers and/or the oriented moments in the ordered state, exists in compound **1**; (3) at 300 K, the b axis is the one with the largest magnetization; while at low temperature, the largest magnetization is along the a^* axis, which suggests that the canting is along the a^* axis. These results were further confirmed by the susceptibility measurements below. Hereafter, we use the symbol A^B to represent the magnetic parameter A along the direction B (a^*, b, and c axes; p for powder).

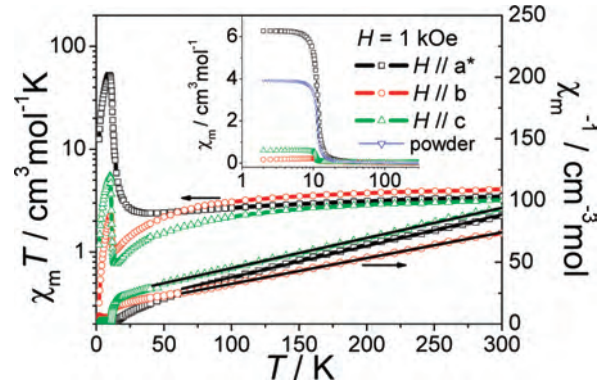

Figure 4. Temperature dependences of the $\chi_m{}^{-1}$, $\chi_m T$, and χ_m (inset) under 1 kOe along the a^*, b, and c axes, together with that for a powder sample. Note that the $\chi_m T$ coordination axis is logarithmic. The lines in the $\chi_m{}^{-1}$ curves are the Curie−Weiss fits.

dc Magnetic Susceptibility and Magnetization. All the experiments below were performed on the crystal of 0.78 mg. Despite the small size of the single crystal, the magnetic signals are fairly good: the moment at 300 K is about 2.0×10^{-5} emu with a standard deviation of 1.6×10^{-7} emu. The temperature dependent susceptibilities along a^*, b, and c were measured and depicted as $\chi_m(T)$, $\chi_m T(T)$, and $\chi_m{}^{-1}(T)$ in Figure 4, together with $\chi_m{}^p$. All χ_m curves increase slowly as the temperature decreases from 300 K, rise abruptly at about 12 K, and stay almost constant from 10 to 2 K, showing spontaneous magnetization (inset of Figure 4). At 300 K, the observation of $(\chi_m T)^b > (\chi_m T)^{a^*} \approx (\chi_m T)^c$ is consistent with the rotation measurement. Curie−Weiss fitting of $\chi_m{}^{-1}$ data above 60 K gives $C^{a^*} = 3.94$, $C^b = 4.80$, $C^c = 4.10$ cm^3 mol^{-1} K (the Curie−Weiss-based g values are $g^{a^*} = 2.90$, $g^b = 3.20$, and $g^c = 2.96$) and $\theta^{a^*} = -48.9$, $\theta^b = -56.2$, and $\theta^c = -85.5$ K. The g values are quite different from a spin only value because of the big orbital contribution. The negative Weiss constants indicate the strong anisotropic AF interaction and the spin−orbital coupling

(24) (a) Carlin, R. L. *Magnetochemistry*; Springer-Verlag: Berlin, 1986; p 317. (b) Mitra, S.; Gregson, A. K.; Hatfield, W. E.; Weller, R. R. *Inorg. Chem.* **1983**, *22*, 1729.

(25) The angle difference, 2.35°, between the a and a^* axes is small, and this could not be identified by the rotation measurement. The minima were presumed along a*.

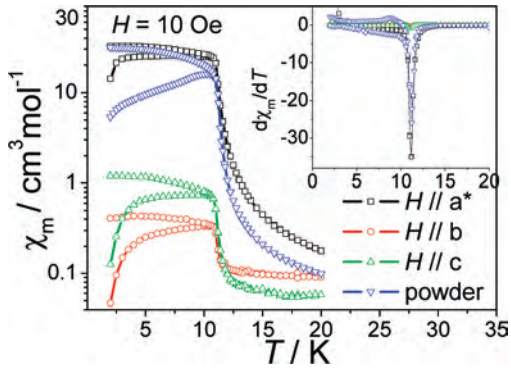

Figure 5. ZFCMs and FCMs of **1** along the a^*, b, and c axes together with those of a powder sample. Note that the χ_m axis is logarithmic. Inset: the derivatives of all the ZFCM/FCM curves.

along three axes. All $\chi_m T$ decrease at high temperature as $(\chi_m T)^p$, but $(\chi_m T)^b$ decreases faster than $(\chi_m T)^{a^*}$ and $(\chi_m T)^c$. It crosses $(\chi_m T)^{a^*}$ and $(\chi_m T)^b$ at about 60 K, and in the range of 60 to 13 K it is between $(\chi_m T)^{a^*}$ and $(\chi_m T)^c$. This should be due to the establishment of the short-range ordering. Below the critical temperature of about 12 K, $(\chi_m T)^b$ becomes smaller than $(\chi_m T)^{a^*}$ and $(\chi_m T)^c$ ($(\chi_m T)^{a^*} > (\chi_m T)^c > (\chi_m T)^b$). It is obvious that the spontaneous magnetization below T_c is strongest along a^* because $(\chi_m T)^{a^*}$ is two orders of magnitude larger than the other two, which confirms again that the canting is along the a^* axis. All these data show the strong magnetic anisotropy in **1**, but it is more complicated than the simple easy axis (Ising) or easy plane (XY) types.

The ZFCM/FCMs (zero-field-cooled and field-cooled magnetization, $H = 10$ Oe, Figure 5) along three magnetic axes also confirmed the above-mentioned aspects. The basic characteristics of FCMs are the same as $\chi_m(T)$ under $H = 1$ kOe with big spontaneous magnetization at low temperature; and all ZFCMs have round peaks and diverge with FCMs at around 10 K. We noticed that following the ZFCM curves on warming, the difference between the ZFCM and FCM is large below about 4 K, and the magnetization quickly reaches almost the saturated value and keeps constant up to the bifurcation temperature. This behavior means that the movement of the magnetic domains is restricted at low temperatures below 4 K. When the temperature is increased, the thermal energy is comparable to the dipolar field, and the domains are aligned along the external field. The fact that the magnetization is saturated well below the bifurcation temperature also means that the moments are almost aligned within the layers because of the strong AF coupling. At around 4 K, the movement of the domain walls might lead to some dynamic behavior, which is reflected in the ac susceptibility measurements with frequency dependent peaks centered around 4 K (vide post). The derivative curves of all ZFCM/FCM have sharp peaks at 11.2 K (inset of Figure 5), which defines its T_C for the long-range ordering.

Furthermore, the isothermal magnetization $M(H)$ at 20 and 2 K (Figure 6a) and the detailed magnetic hysteresis loops at 2 K (Figure 6b) were measured in all three directions. At 20 K, all $M(H)$ curves increase almost linearly up to 50 kOe with $M^{a^*} > M^p > M^b > M^c$, consistent with the paramagnetic state and the above anisotropic results. Meanwhile at 2 K,

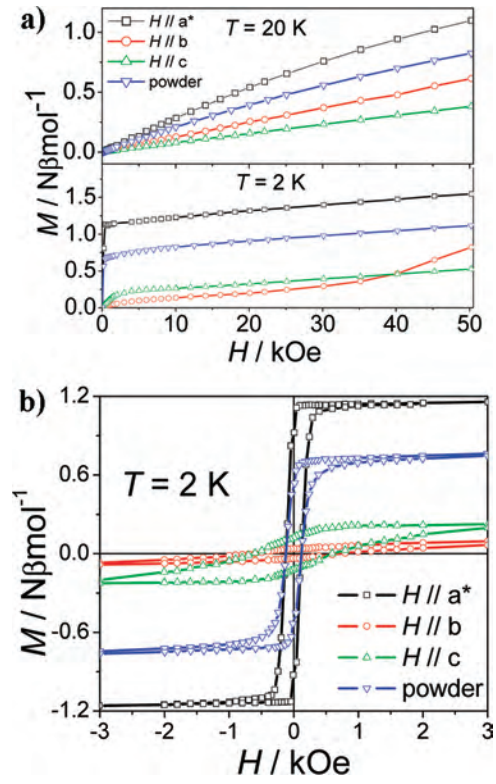

Figure 6. (a) Field dependent magnetization at 20 and 2 K and (b) the magnetic hysteresis loops at 2 K along the a^*, b, and c axes and that for a powder sample.

M^{a^*} increases rapidly at very low field and then slowly increases to 1.54 μ_B at 50 kOe. M^b and M^c are much smaller than M^{a^*}. For M^b, it increases slowly until 30 kOe where it is 0.29 μ_B, and then goes quickly to 0.82 μ_B at 50 kOe. For M^c, it is larger than M^b below 40 kOe and smaller thereafter with 0.53 μ_B at 50 kOe. It looks like there is a field induced spin-flip along the b axis. Apparent hysteresis loops can be observed at 2 K in all measurements. The remnant magnetizations are $M_R^{a^*}(1.13\ \mu_B) > M_R^p(0.54\ \mu_B) > M_R^c(0.12\ \mu_B) > M_R^b(0.037\ \mu_B)$ and the coercive fields are in the reverse order, $H_c^{a^*}(120\text{ Oe}) \approx H_c^p(120\text{ Oe}) < H_c^c(600\text{ Oe}) < H_c^b(800\text{ Oe})$. These $M(H)$ results clearly indicate that the a^* axis is the direction of residue moments in the ferromagnetic-like ordered state.

ac Magnetic Susceptibilities. To further characterize the ground-state at low temperature, ac susceptibilities at zero dc field were measured, both for the powder samples and for the single crystal with field parallel to a^* (Figure 7a and 7b, $f = 3.16-1000$ Hz). As we can see, the ac signals for both are very strong and show similar behaviors. On decreasing temperature, the in-phase signals χ_m' behave similarly to the ZFC curves: increase abruptly at around 11 K, reach the maximum at about 10.8 K, and then decrease slowly toward zero. The out-of-phase signals χ_m'', on the other hand, have nonzero values at about 11 K, increase steadily to the maximum around 4−6 K, and then decrease slowly. The $d(\chi_M'T)/dT$ curves all have peaks at $T_C = 11.2$ K, consistent with the dc measurements. Although there is no frequency dependence for both the χ_m' and χ_m'' at around T_C, obvious frequency dependence was observed at lower temperatures for both samples. The temperature of

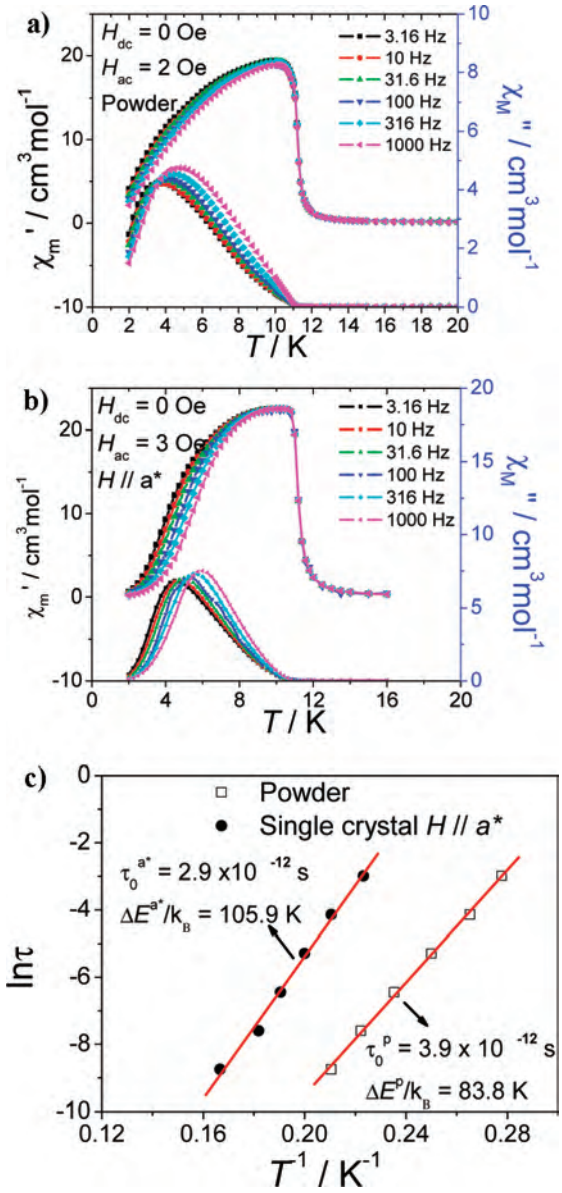

Figure 7. Temperature dependent ac susceptibility of **1** in a zero applied static field in the frequency range of 3.16−1000 Hz for (a) the powder sample and (b) the single crystal sample with the field parallel to *a**. The Arrenius fits of the two sets of data are displayed in (c).

the peaks T_p in χ_M'' moves from 3.5 to 4.75 K for the powder (4.5 to 6.0 K for the single crystal) with frequency from 3.16 to 1000 Hz. The shift parameter $\phi = (\Delta T_p/T_p)/\Delta(\log f)$ is about 0.12 for both, which is indicative to a slow magnetic relaxation and is very close to the value of the superparamagnetic materials like the SMM and SCM.[26] (The χ_m' should be used to calculate ϕ; however, we use the χ_m'' here because they have obvious peaks).

The Arrenius law, $\tau = \tau_0 \exp(\Delta E/k_B T)$, can be used to fit the ac data for both samples to give an estimate of the magnetic relaxation (Figure 7c). As can be seen, there is a small difference between the powder and the single crystal. The pre-exponential factors τ_0 are of the same order, with $\tau_0^p = 3.9 \times 10^{-12}$ s and $\tau_0^{a^*} = 2.9 \times 10^{-12}$ s, respectively. However, the energy barriers for the relaxation $\Delta E/k_B$ are $\Delta E^p/k_B = 83.8$ K and $\Delta E^{a^*}/k_B = 105.9$ K. All these values are similar to a superparamagnet.[26] However, this relaxation behavior is more complicated. We tried to measure the Cole−Cole plots for the powder sample at different temperatures (3, 3.5, 4, 4.5, and 5 K, Supporting Information, Figure S1). Only that at 3 K shows an irregular semicircle, and it can not be fitted with the Debye model to a reasonable α value, indicating a very large distribution of the relaxation time. Because there are no disordered components and competitive interactions in the structure and the relaxation behavior can be observed in one single crystal, the relaxation should not come from the spin-glass state. We presume that the slow relaxation behavior might come from the movement of the domain walls[27] and/or the orbital liquid behavior[28] caused by the residual orbital magnetization. As discussed above in the ZFCM/FCM part, the movement of the domain walls is very likely responsible for this dynamic behavior because the frequency dependence is obvious only at low temperature around 4 K, the same temperature range where the ZFCM increases quickly to the saturated value. More thorough study on these spin dynamics is needed to fully understand the physical properties of **1**. The bigger $\Delta E^{a^*}/k_B$ value for the single crystal suggests that the movement of the domain walls in a single crystal is more difficult than that in a powder. The ac signals with field along the other two directions are too weak and not measured.

Discussions

Now, we can conclude several fundamental aspects of the magnetic property of **1**: strong *AF* coupling between the adjacent Co^{2+} is transmitted through the *EE* azido; because of the orbital residue and strong spin−orbital coupling of octahedral Co^{2+}, strong magnetic anisotropy exists in **1**, even at room temperature; short-range ordering starts to be established well above T_c, and large spontaneous magnetization emerges below T_c. The spontaneous magnetization could arise from a ferrimagnet or a weak-ferromagnet with a large canting angle in an *AF* coupled system. Because it is impossible to generate a ferrimagnetic lattice in **1** with only one unique Co^{2+} center, we attribute its behavior to a weak-ferromagnet with a large canting angle. The real spin should be along the *b* axis because the magnetization is largest along *b* at room temperature; the resulting net moment should be along *a** as suggested by the fact that the spontaneous magnetization is largest along *a**. Thus, we may propose a spin configuration in the ordered state (Figure 8). The spins are antiparallel to each other and stay mainly in the *bc* plane

(26) (a) Mydosh, J. A. *Spin Glasses: an Experimental Introduction*; Taylor & Francis:London, 1993; (b) Binder, K.; Young, A. P. *Rev. Mod. Phys.* **1986**, *58*, 801. (c) Etzkorn, S. J. Magnetic Relaxation in Organic-Based Magnets. Ph.D. Thesis. The Ohio State University, Columbus, Ohio, 2003.

(27) Haase, W.; Wróbel, S. *Relaxation Phenomena: Liquid Crystals, Magnetic Systems, Polymers, High-Tc Superconductors, Metallic Glasses*; Springer-Verlag: New York, 2003.

(28) (a) Khaliullin, G.; Maekawa, S. *Phys. Rev. Lett.* **2000**, *85*, 3950. (b) Fritsh, V.; Hemberger, J.; Büttgen, N.; Scheidt, E. W.; Krug von Nidda, H. A.; Loidl, A.; Tsurkan, V. *Phys. Rev. Lett.* **2004**, *92*, 116401. (c) Feiner, L. F.; Oles, A. M.; Zaanen, J. *Phys. Rev. Lett.* **1997**, *78*, 2799. (d) Ishihara, S.; Yamanaka, M.; Nagaosa, N. *Phys. Rev. B* **1997**, *56*, 686. (e) Khomskii, D. I.; Mostovoy, M. V. *J. Phys. A* **2003**, *36*, 9197.

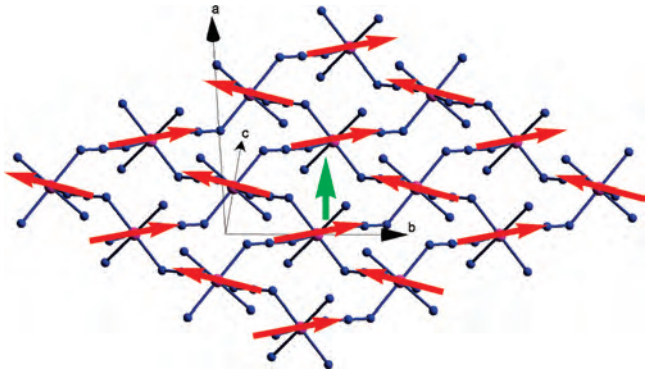

Figure 8. Proposed spin configuration of **1**. The red arrows represent individual moments of Co^{2+} and the green arrow represents the net moment, which is along the a^* axis and perpendicular to the bc plane.

along the b axis. At the same time, they incline out of the plane with an angle γ, as leads to the net moments along a^*. These net moments along a^* in the adjacent layers should be then weakly ferromagnetically coupled, leading to the final spontaneous magnetization of **1**. The weak interlayer ferromagnetic exchange might come from the dipole−dipole interaction. Along b, no net moment is formed, and it is the $\chi_{//}$ direction in an antiferromagnet. This explains the fact that ${\chi_m}^b$ is the smallest below T_c. The canting angle γ at 2 K can be estimated through the equation $\sin(\gamma) = {M_R}^{a^*}/{M_S}^4$ ($M_S = g^{a^*}SN\beta = 4.35\ \mu_B$, where $S = 3/2$, $g^{a^*} = 2.90$) to be up to 15°. (From the remnant magnetization ${M_R}^p$ of the powder sample, the canting angle of **1** at 2 K can also be roughly estimated to be 15°. For octahedral Co^{2+} at 2 K, the effective spin of $S = 1/2$ is used with a common value of $g = 4.3$.)

1 demonstrates the possibility to generate the weak-ferromagnets with big spontaneous magnetization. For the sake of "rational design", perception of the origin of spin-canting is necessary. Generally, spin-canting can arise from two different sources, the antisymmetric magnetic exchange (Dzyaloshinsky−Moriya (DM) interaction), which requires the lack of an inversion center between the adjacent spins, and the magnetic anisotropy.[8,9] It has been proved that the more anisotropic the system is, the bigger the canting will be. Because the canting angle is very high and up to 15°, it is very unlikely that the canting is from the DM interaction alone. The anisotropy field, such as the interlayer dipolar field, should play a very important role in this phenomenon. On the basis of our series results,[10,18] we would like to argue the relationship of spin-canting to the chemical character of the bridges. At the very beginning, canting was observed in some materials with spins *AF* coupled through a single-atom bridge such as O (Fe_2O_3), Cl ($CsCoCl_3 \cdot 2H_2O$), S (β-MnS), and so forth.[29] Provided that ∠M−X−M is not 180° and there is only one bridging X atom between M centers, atom X will always exclude the inversion center between the bridged two spins and symmetrically favor the spin-canting. Similarly, the canting was also frequently observed in *AF* materials bridged by some three-atom bridges such as N_3^-,[10,11] $N(CN)_2^-$ (of 1,3 mode),[12,13] pyrimidine[14,15] and $HCOO^-$,[16,18] because of the same symmetry reason.

In light of above considerations, we proposed here the weak-ferromagnetic strategy for the construction of molecular magnets of big spontaneous magnetization. This approach should have the following important aspects. First, strong *AF* interactions are obviously needed to increase the critical temperature. Second, the system should be symmetrically allowed for the spin-canting. The adjacent spins cannot be related by an inversion center. This requirement can be partially realized by choosing those acentric bridges ($HCOO^-$, pyrimidine, $NHCN^-$, dca^-, and so forth) or those that can exclude the inversion centers (e.g., the single-bridged O^{2-}, S^{2-}, halogen, and N_3^-). Third, because the DM interaction and the degree of spin-canting are proportional to the anisotropy, those ions with strong single-ion anisotropy, like Co^{2+}, Mn^{3+}, Fe^{2+}, $Cr^{2+,}$ and V^{2+}, are preferred. Although the strength of the DM interaction and the degree of the magnetic anisotropy are not really something one can design, these considerations still will increase the chances to get a weak-ferromagnet with big canting. Actually, these are the exact conditions satisfied in **1** and in those several examples with big canting angles and spontaneous magnetizations.

Summary

Through detailed measurements on both powders and well oriented single crystal, the magnetic properties of an *EE*-azido bridged cobalt compound $Co(N_3)_2(4acpy)_2$ were carefully studied. This compound shows the phase transition from paramagnetic to long-range ordered weak-ferromagnetic state at $T_c = 11.2$ K. Strong magnetic anisotropy at both room temperature and below T_c, big spontaneous magnetization, and unusual magnetic slow relaxation below T_c were observed. The possible spin configuration consistent with the experiments was proposed. The big spontaneous magnetization was attributed to the very big canting angle in the weak-ferromagnetic state. The origin of the spin canting was discussed; on the basis of this, the weak-ferromagnetic strategy for the synthesis of molecular magnets with large and permanent magnetization was proposed. Although the studies on the single crystal revealed a lot of information, more thorough work is still needed to fully understand the nature of its ground state.

Acknowledgment. We acknowledge the support of the National Natural Science Foundation of China (No.ʼs 20221101, 20490210, and 20571005), the National Basic Research Program of China (2006CB601102), and the Research Fund for the Doctoral Program of Higher Education (20050001002).

Supporting Information Available: X-ray crystallographic CIF file for **1**, and the Cole−Cole diagram at different temperatures (PDF). This material is available free of charge via the Internet at http://pubs.acs.org.

IC7023549

(29) (a) Morin, F. J. *Phys. Rev.* **1950**, *78*, 819. (b) Worlton, T. G.; Decker, D. L. *Phys. Rev.* **1968**, *171*, 596. (c) Kopinga, K.; van Vlimmeren, Q. A. G.; Bongaarts, A. L. M.; de Jonge, W. J. M. *Physica B+C* **1977**, *671*, 86–88. (d) Keffer, F. *Phys. Rev.* **1962**, *126*, 896.